
Towards the Practical Utility of Federated Learning in the Medical Domain

**Seongjun Yang[†], Hyeonji Hwang[†], Daeyoung Kim[†], Radhika Dua[†],
Jong-Yeup Kim[‡], Eunho Yang[†], Edward Choi[†]**

[†]Korea Advanced Institute of Science and Technology,

[‡]Department of Biomedical Informatics, College of Medicine, Konyang University

{seongjunyang, localh, daeyoung.k, radhikadua, eunhoy, edwardchoi}@kaist.ac.kr,
jykim@kyuh.ac.kr

Abstract

Federated learning (FL) is an active area of research. One of the most suitable areas for adopting FL is the medical domain, where patient privacy must be respected. Previous research, however, does not fully consider who will most likely use FL in the medical domain. It is not the hospitals who are eager to adopt FL, but the service providers such as IT companies who want to develop machine learning models with real patient records. Moreover, service providers would prefer to focus on maximizing the performance of the models at the lowest cost possible. In this work, we propose empirical benchmarks of FL methods considering both performance and monetary cost with three real-world datasets: electronic health records, skin cancer images, and electrocardiogram datasets. We also propose Federated learning with Proximal regularization eXcept local Normalization (FedPxN), which, using a simple combination of FedProx and FedBN, outperforms all other FL algorithms while consuming only slightly more power than the most power efficient method.

1 Introduction

Federated learning (FL) is a distributed machine learning framework in which each client does not share its data, but instead shares model parameters, thus preserving data privacy. The local models are trained in each local device, sent to the trusted global server, and aggregated. The aggregated global model is then sent back to each local client. By iterating such communication, the global server can provide each client with a model that is better than a model solely trained by an individual client. FL is divided into cross-device and cross-silo FL [16, 46]. Typically, mobile devices are the clients in a cross-device setting, and hence this scenario has a considerable number of clients. The critical factors in the cross-device setting are the Internet connectivity and the efficiency of training in each device because a mobile device usually uses Wi-Fi, and the efficiency will affect its battery. However, in the cross-silo setting, in which silos such as hospitals are the clients, Internet connectivity is not critical because the silos often use LAN connections [16]. However, when it comes to the training, efficiency still matters in the cross-silo setting because of training costs such as GPU cloud fees or the electricity bill.

Recently, researchers have begun to test FL on the medical datasets with varying success [5, 9, 22, 27, 39, 40]. However, existing studies do not fully consider the real-world needs of those who are most likely to use FL in the medical domain. It is not the hospitals who are actively seeking to adopt FL, because hospitals that can afford to adopt advanced machine learning technologies typically possess large data, which is usually sufficient for meeting their individual needs. It is rather service providers such as large IT companies or startups who want to develop machine learning models with real patient records via FL, in order to create services such as providing predictive models to multiple hospitals

or consumers. These likely users (i.e., IT companies) will care about two things when determining which FL algorithm to use: model performance and monetary cost (i.e., power consumption).

In this work, for the first time, we test well-known FL algorithms proposed by the machine learning community on three medical datasets in order to evaluate their utility in terms of both performance and monetary cost. Specifically, we select basic FL algorithms as well as those designed for heterogeneous data distributions among different clients (i.e., hospitals). We test all algorithms on the three representative real-world medical datasets with different modalities involving structured (i.e., tabular), visual, and signal data as follows:

- Longitudinal electronic health records (eICU) [35] collected from multiple hospitals in the US for six clinical prediction tasks such as mortality prediction and length-of-stay prediction;
- Medical images, specifically skin images collected by five institutions from multiple countries for diagnosing multiple skin cancer types;
- Electrocardiogram signals collected from five institutions from multiple countries, for diagnosing diverse heart conditions.

Furthermore, because of the different data distributions provided by clients, we study the effect of using different normalization strategies in each task and how they affect the performance of different FL algorithms. We also calculate the power consumption needed by each FL algorithm for all three datasets to estimate their approximate monetary cost. In addition, based on our observation of how the parameters behave during training in FedProx [24] and FedBN [26], we propose a new hybrid FL algorithm, FedPxN, which combines the strength of both algorithms. An evaluation of FedPxN using the same set of experiments confirms that our method consistently outperforms all FL algorithms in all three datasets and requires marginally increased power consumption.

2 Related work

FL algorithms on data that are not independent and identically distributed (i.i.d.). The main challenge of FL in the medical domain is a non-i.i.d. problem [39, 23] because of factors such as different specific protocols, medical devices, and local demographics. Hence, we review FL methods that handle data heterogeneity. However, FedAvg [31], a widely known framework in FL, does not ensure training convergence when data are heterogeneous over local clients [25, 13]. Therefore, a large number of methods focus on addressing the non-i.i.d. problem. FedProx [24] adds a proximal term in the local objective of the FedAvg framework to solve the heterogeneity problem, and FedOpt [36] applies adaptive optimization in global aggregation to stabilize convergence for heterogeneous data. The inconsistency of local and global objectives due to the data heterogeneity of each local client is handled in Scaffold [18] and FedDyn [1]. Scaffold computes and aggregates control variates, whereas FedDyn uses a dynamic regularizer to solve the problem. Most FL methods [31, 24, 36, 18, 1] are validated in a label-heterogeneous experimental setting by partitioning the same sourced dataset into multiple clients. In contrast, FedBN [26] considered the non-i.i.d problem that can occur due to feature shifts in different data sources, and proposed to aggregate local models without batch normalization layers to handle this problem. Similarly, SiloBN [2] aggregates local models without local batch normalization statistics.

FL in Healthcare The medical domain is an active area of FL nowadays because of the importance of patient privacy. Prior study on FL in the medical domain [22] has achieved performance comparable to that of centralized learning. However, these studies focused only on electronic health records (EHR), and electrocardiogram (ECG) signals. Moreover, they randomly sample the data to create heterogeneity. However, in reality, heterogeneity also exists in the feature space. In our work, we focus on diverse and important modalities in healthcare (images, EHR, and ECG) and also consider a realistic scenario in which the clients are from different hospitals. Effective FL frameworks for specific tasks have been empirically demonstrated for each specific modality such as EHR and medical images in [14, 20, 28, 34, 49]. However, these results depended on architecture or were validated only on specific modalities.

Normalization layer for FL In [8, 12], the authors compared performance when using various normalization layers in the local model for image classification tasks. Our study observes which normalization is effective in eight clinical tasks.

3 Methods

FL methods are often designed to minimize the weighted average of local objective function of clients as follows:

$$\min_w F(w) := \sum_{k=1}^K \frac{n_k}{n} F_k(w), \quad (1)$$

where K is the number of clients, n_k the number of examples in each client k , n the total data size of all clients, and F_k the local objective function of each client k . Data heterogeneity is a key and common challenge in solving Eq. 1. In this section, we describe the popular FL methods for solving data heterogeneity, that are evaluated in the experiments. In addition, we propose a new FL method (FedPxN) based on the analysis of the different training patterns of the parameters of each client in FedBN [26] and deployment of the proximal term [24].

Algorithm 1: Federated Averaging

Input: number of clients K , number of communication rounds T , number of local epochs E ,
 Data $D := (D_1, D_2, \dots, D_K)$, learning rate η
Output: model parameter w_T

```

1 Server executes:
2   initialize model parameters  $w_0$ 
3   for  $t = 0, \dots, T - 1$  do
4     for each client  $k \in K$  do
5        $w_{t,k} \leftarrow w_t$ 
6        $w_{t,k} \leftarrow \text{LocalTraining}(k, w_{t,k}, D_k)$ 
7     end
8      $w_{t+1} \leftarrow \sum_{k=1}^K \frac{n_k}{n} w_{t,k}$ 
9   end
10  LocalTraining( $k, w_{t,k}, D_k$ ):
11    for  $e = 0, \dots, E - 1$  do
12      for batch  $b \leftarrow (x, y)$  of  $D_k$  do
13         $w_{t,k} \leftarrow w_{t,k} - \eta \nabla F_k(w_{t,k}; b)$ 
14      end
15    end
16    return  $w_{t,k}$ 

```

3.1 FedAvg

Federated averaging (FedAvg) [31] is the de facto standard algorithm in FL (Algorithm 1). In this framework, first, the central server sends the global model w_t to the clients in each communication round t (line 5). Then, each client k sends the updated model $w_{t,k}$ back to the server after local training (line 6). Next, the central server averages all client models considering the data size ratio n_k/n (line 8). Unlike distributed stochastic gradient descent [31], FedAvg reduces the number of communication rounds required for model convergence by updating the model after multiple epochs E of local training. Most FL algorithms today are derived from FedAvg. Every baseline of our work is also based on FedAvg, so we use the notation used in FedAvg for describing other methods.

3.2 FedProx

To solve the non-i.i.d problem, FedProx [24] introduces an L_2 regularization term $\|w_{t,k} - w_t\|_2^2$ to the local objective function F_k of the FedAvg framework as follows:

$$\tilde{F}_k(w_{t,k}; b) = F_k(w_{t,k}; b) + \frac{\mu}{2} \|w_{t,k} - w_t\|_2^2, \quad (2)$$

where F is the objective function and μ is a hyperparameter that controls the degree of regularization. The local model updates are restricted by the regularization term so that they are closer to the global model.

3.3 FedBN

In FedBN [26], the local models are aggregated without batch normalization layers in order to handle feature shifts among clients. The study [26] evaluated FedBN’s effectiveness through experiments using datasets from different sources. In our study, we use different types of normalization (i.e., batch normalization (BN) [15], group normalization (GN) [48], and layer normalization (LN) [3]) for each task to maximize the performance of the models. Hence, we extend FedBN in such a way that all layers of the local models except the normalization layers are aggregated.

3.4 FedOpt

FedOpt [36] applies adaptive optimization to model the aggregation stage in FedAvg. First, the pseudo gradient $\Delta_{t,k} := w_{t,k} - w_t$ of each client k is calculated after local training at each round t . Second, it calculates Δ_t by averaging each pseudo gradient $\Delta_{t,k}$. Third, the momentum $m_t \leftarrow \beta_1 m_{t-1} + (1 - \beta_1) \Delta_t$ is calculated. Then, v_t is calculated using different adaptation techniques (FedAdam, FedAdagrad, FedYoGi) as follows:

$$\begin{aligned} v_t &\leftarrow \beta_2 v_{t-1} + (1 - \beta_2) \Delta_t^2 && \text{FedAdam,} \\ v_t &\leftarrow v_{t-1} + \Delta_t^2 && \text{FedAdagrad,} \\ v_t &\leftarrow v_{t-1} - (1 - \beta_2) \Delta_t^2 \text{sign}(v_{t-1} - \Delta_t^2) && \text{FedYoGi,} \end{aligned} \quad (3)$$

where β_1, β_2 are the hyperparameters for adaptation. Finally, a global model is updated using m_t and v_t as follows:

$$w_{t+1} \leftarrow w_t + \eta_g \frac{m_t}{\sqrt{v_t} + \gamma}, \quad (4)$$

where η_g is the server learning rate and γ represents the degree of adaptivity for each algorithm.

3.5 FedDyn

In FedDyn [1], the local model $w_{t,k}$ is updated by adding a penalized risk function to the objective function F_k of FedAvg during local training. The risk objective of each client is dynamically updated using both local and global model as:

$$\hat{F}_k(w_{t,k}; b) = F_k(w_{t,k}; b) - \langle \Delta F_k(w_{t-1,k}; b), w_{t,k} \rangle + \frac{\alpha}{2} \|w_{t,k} - w_{t-1}\|^2, \quad (5)$$

where α is the hyperparameter controlling the degree of regularization. Theoretically, local models converge to the global model if they converge in local training of FedDyn.

3.6 Proposed Framework: FedPxN

Because the statistics used in the normalization layers are different in each local client $w_{t,k}$, it could be challenging for the aggregated model w_t to capture the distribution of data collected from different sources. A simple solution to this problem is to aggregate the local client models without the normalization layers, as in FedBN.

The normalization layers in FedBN naturally move towards their own local optimum depending on the data distribution of each client. However, we suspect that the other non-normalization layers might also move towards the local optimum inconsistent with the global optimum because of the effect of the normalization layers in the model of each client. Therefore, we measure the L_2 distance between all $w_{t,k \setminus \text{norm}}$, and $w_{t \setminus \text{norm}}$, where the former are the local model parameters except for the normalization layers in client k , and the latter are the global model parameters except the normalization layers in each round t , as follows:

$$\|w_{t,k \setminus \text{norm}} - w_{t \setminus \text{norm}}\|_2^2, \quad (6)$$

where t indicates each communication round, k denotes each local client. As shown on the left side of Figure 1, each client’s model $w_{t,k \setminus \text{norm}}$ has evolved in different directions from the global model $w_{t \setminus \text{norm}}$. Therefore, we hypothesize that a proximal term (Equation 6) inspired by FedProx will help the local models in FedBN to progress towards the global optimum. As the right side of Figure 1 shows, the added proximal term prevents $w_{t,k \setminus \text{norm}}$ from deviating too much from $w_{t \setminus \text{norm}}$.

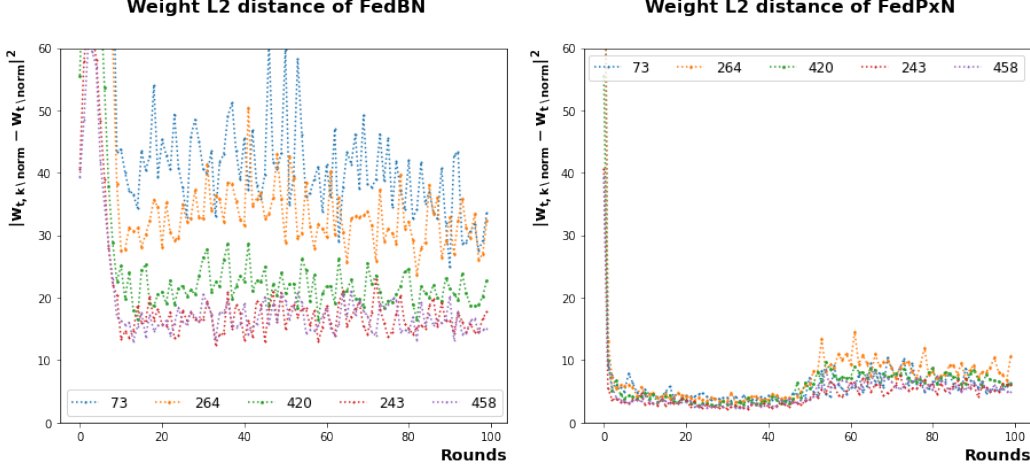


Figure 1: L_2 distance between each client’s model parameters and the global parameters, excluding the normalization layers, when using FedBN (left) and when using FedPxN (right), which regularizes all local model parameters besides those in the normalization layers. Both show results of the mortality prediction task, in which all models were equipped with layer normalization, and trained using the five clients with the largest EHR training samples.

Algorithm 2: Federated learning with Proximal regularization eXcept local Normalization (FedPxN)

Notation: number of clients K , number of communication rounds T , number of local epochs E , Data $D := (D_1, D_2, \dots, D_K)$, learning rate η , normalization layers $norm$

```

1 Server executes:
2   initialize model parameters  $w_0$ 
3   for  $t = 0, \dots, T - 1$  do
4     for each client  $k \in K$  do
5        $w_{t,k}\backslash norm \leftarrow w_{t\backslash norm}$ 
6        $w_{t,k} \leftarrow \text{LocalTraining}(k, w_{t,k}, D_k)$ 
7     end
8      $w_{t+1}\backslash norm \leftarrow \sum_{k=1}^K \frac{n_k}{n} w_{t,k}\backslash norm$ 
9   end
10 LocalTraining( $k, w_{t,k}, D_k$ ):
11   for  $e = 0, \dots, E - 1$  do
12     for batch  $b \leftarrow (x, y)$  of  $D_k$  do
13        $R = \|w_{t,k}\backslash norm - w_{t\backslash norm}\|^2$ 
14        $w_{t,k} \approx \arg \min_w F_k(w; b) + \frac{\mu}{2} R$ 
15     end
16   end
17   return  $w_{t,k}$ 

```

Based on this observation, we propose FedPxN, an algorithm encouraging the normalization layers to adapt to each client’s unique feature distribution and the other layers to follow the global optimum in order to improve the overall performance. In FedPxN, local models are updated by the local objective with the proximal term of the other layers of the global model during local training and then aggregated without the normalization layers. The detailed algorithm is presented in Algorithm 2.

4 Experimental Setup

In this section, we introduce the different medical datasets and experimental settings used to evaluate all FL frameworks for the medical domain in terms of their practical utility. For all our experiments, we assumed the full participation of clients in all communication rounds by LAN connection. For

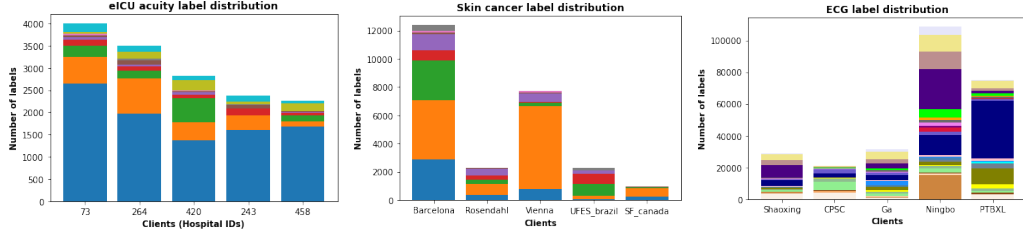


Figure 2: Label distributions of eICU, skin cancer images, and ECG. Colors indicate the labels for each client. The label distribution shown for eICU is for the final acuity prediction task for the five clients with the largest datasets.

all FL methods in each of the tasks in our study, we used the same deep learning model, data size, input size, and GPU (NVIDIA Geforce RTX 3090) in order to conduct a fair comparison among them. Further, we fixed the total number of training epochs for each local client in all FL methods, where this number is defined as the number of local epochs times the number of communication rounds. This implies that the total FLOPs and the theoretical computation cost are similar for all FL methods, increasing the fairness of the comparison. We conducted the experiments by setting various communication rounds and local epochs. For each dataset, the total number of training epochs was set to 100, 300 and 200 respectively, which was sufficient for all models using all FL methods to converge. After training, among model weights from all communication rounds w_1, \dots, w_T , the w_t that showed the best average validation performance across all clients is chosen as the final model weight. Then we use the final model weight to calculate the average test performance across all clients. We repeated all experiments three times and report the mean test performance.

4.1 eICU database

We first evaluated FL methods on the eICU dataset by taking advantage of an available benchmark dataset [30], which consists of intensive care unit (ICU) records of patients aged 15 years or over. The benchmark dataset in [30] contains labs, vitals, and demographic information. The labs and vitals were measured for at least 5% of all observed time-points. The benchmark dataset contains 71477 ICU stays across 59 hospitals, where ICU stays range between 540 and 4008 for each hospital. To conduct experiments in the FL setting, we used the 5, 10, 20, and 30 hospitals with the most ICU stays (with total of 14962, 25198, 39501, and 50434 ICU stays) and performed the following six clinical prediction tasks:

- **Mortality prediction** (mort_24h, mort_48h)
 This task aims to predict whether the recorded time of death is within 24/48 hours.
Input: first 24 hours of data;
Type: binary classification.
- **Length-of-stay prediction** (LOS)
 The LOS task aims to predict whether the patient’s total stay is more than three days.
Input: first 24 hours of data;
Type: binary classification.
- **Discharge prediction** (disch_24h, disch_48h)
 This task predicts whether the patient is discharged within the next 24/48 hours. If the patient is discharged, this task further aims to predict the next place of the patient (e.g., a skilled nursing facility or home).
Input: first 24 hours of data;
Type: 10-way classification.
- **Final acuity prediction** (Acuity)
 This task aims to predict whether a patient dies or is discharged. If the patient dies, it also predicts when the patient dies (e.g., in ICU or in hospital). If the patient is discharged, this task also aims to predict the next place of the patient.
Input: first 24 hours of data;
Type: 10-way classification.

Among all tasks that have heterogeneous label distribution, as an example, we show the label distribution of the Final acuity prediction task in the left plot of Figure 2. While the most dominant label is shared by all clients, the label distributions and data volumes vary across the clients. We used a 2-layer Transformer encoder model [45] followed by two fully connected (FC) layers, similar to [41]. We also applied Layer Normalization (LN) between the FC layers. We conducted additional experiments in which we replaced the LN used in the Transformer encoder and FC layers with Group Normalization (GN). We randomly split the ICU stays of each client using the ratio of 7:1.5:1.5 to form training, validation, and test sets. To train the models for binary classification, and 10-way classification tasks, we used the binary cross-entropy loss and cross-entropy loss, respectively. We used the Adam optimizer [21], a batch size of 256, a single local epoch, 100 communication rounds, and 100 total training epochs in all of the tasks. We tested varying combinations of the number of local epochs and communication rounds, such as 5 & 20 and 10 & 10, but 1 & 100 generally gave the best performance for all FL methods in all tasks. Further details are discussed in Section 5.4. We utilized the AUROC and AUPRC scores to evaluate the performance of the trained model. Please refer to the GitHub repository [10] for the AUPRC score and more details on the training of the different FL methods.

4.2 Skin cancer dataset

We also evaluated all FL methods on skin cancer datasets. Following [6], we used the ISIC19 [7] and HAM10000 [44] datasets, removing image samples that appear in both datasets from the ISIC19 dataset. Then, we split the HAM10000 [44] dataset into two datasets based on the source of the data sample. Hence, we formed three clients from the ISIC19 and HAM10000 datasets. The clients are from the Hospital Clinic de Barcelona (Barcelona), Medical University of Vienna, Austria (Vienna), and Queensland University, Australia (Rosendahl). In addition to these three clients, we formed two more clients, PAD-UFES [33] and Derm7pt [19], following [4]. These two clients are from the Federal University of Espírito Santo, Brazil (UFES_brazil), and Simon Frazer University, Canada (SF_canada). The details of the label distribution and size of the data for each client are shown in the middle plot of Figure 2. We observe that the dominant label is almost the same for all clients and all clients have an imbalanced dataset. Further, we observe that the second dominant label is more different for each client, and the total number of samples significantly varies from one client to another. We split the data of each client into training, validation, and test sets in the ratio of 7 : 1.5 : 1.5.

For this dataset, we formulated an 8-way classification task that uses an image as input and predicts the type of skin cancer. We used either BN or GN and trained an EfficientNet-B0 [43] model for the skin cancer classification task using cross-entropy loss. We also tested LN, but it showed consistently worse performance than BN or GN. To evaluate the performance of the model, we use two metrics, namely AUROC and AUPRC. We used the Adam optimizer, a batch size of 128, a single local epoch, 300 communication rounds, and 300 total training epochs. In our experiments, we resized the input images to $256 \times 256 \times 3$. For more details, please refer to the GitHub repository [10].

4.3 ECG dataset

We also evaluated the FL methods on ECG signals. We used the PhysioNet 2021 [37] dataset and split it into five clients based on the hospital that collected the data sample. The clients are Shaoxing People’s Hospital, China (Shaoxing), CPSC 2018, China (CPSC), Georgia 12-lead Challenge Database, USA (Ga), Ningbo First Hospital, China (Ningbo), and Physikalisch-Technische Bundesanstalt, Germany (PTBXL). Following [32], we extracted samples with a sampling frequency 500Hz and divided the data into 5-second segments.

Our aim is to solve a multi-label prediction task in which a 12-lead ECG sample is given as input, and the objective is to diagnose 26 types of cardiac diseases. In Figure 2, the label distribution of different clients for these data reveals that the total number of samples varies substantially from one client to another, and the data are imbalanced. Moreover, the dominant label in the data from each client varies. We randomly split the data in the ratio of 8:1:1 to form training, validation and test sets. We used asymmetric loss [38] and trained a ResNet-NC-SE [17] because it showed the best performance on 12-lead ECG readings in PhysioNet 2021 to the best of our knowledge [11, 47]. We also conducted experiments in which we added either BN or GN. We used the AdamW optimizer [29], a batch size of 64, a single local epoch, 200 communication rounds, and 200 total training epochs.

For the FedOpt-based methods, we only report the results of FedAdam for the ECG experiments because the other FedOpt-based methods, FedAdagrad and FedYoGi, showed similar performance, as in the eICU and skin cancer experiments. Following [32], we evaluated the performance of our approach by measuring the CinC score, the official evaluation metric used by the Physionet 2021 challenge that takes into account domain knowledge on cardiovascular diseases. For more details, please refer to the GitHub repository [10].

5 Experimental Result

5.1 Results for eICU

Table 1: AUROC results for the eICU dataset using the data of the five largest clients. For each FL method, bold indicates the better normalization technique (LN or GN). We indicate the highest average AUROC results for all six tasks in blue.

		FedAvg	FedProx	FedBN	FedAdam	FedAdagrad	FedYoGi	FedDyn	FedPxN
mort_24h	LN	67.85 \pm 2.52	73.29 \pm 2.13	69.31\pm0.56	68.27\pm1.98	67.76\pm1.85	60.75 \pm 3.78	70.80\pm0.68	74.05 \pm 1.61
	GN	69.54\pm2.23	74.02\pm2.57	69.05 \pm 1.64	67.60 \pm 2.39	67.21 \pm 0.77	70.82\pm3.57	69.79 \pm 2.09	75.07\pm1.83
mort_48h	LN	68.33\pm3.55	72.37 \pm 1.42	68.38 \pm 0.81	69.61 \pm 1.31	68.62\pm1.47	68.69 \pm 0.56	67.99 \pm 1.23	72.22 \pm 1.87
	GN	67.81 \pm 0.58	72.46\pm1.42	69.42\pm1.08	70.71\pm0.64	68.32 \pm 0.51	70.23\pm0.86	72.64\pm3.11	72.33\pm1.02
LOS	LN	63.23 \pm 0.31	62.97 \pm 0.34	63.04 \pm 0.13	62.46\pm0.40	62.61 \pm 0.57	62.31 \pm 0.71	61.97 \pm 0.53	63.73\pm0.42
	GN	63.61\pm0.24	63.55\pm0.27	63.36\pm0.03	62.36 \pm 0.85	62.83\pm0.65	62.54\pm0.98	63.05\pm1.11	63.68 \pm 0.18
disch_24h	LN	67.58\pm0.40	67.95 \pm 0.56	68.18\pm0.22	66.37\pm1.42	66.50 \pm 0.32	66.26 \pm 1.02	66.99 \pm 0.87	67.98 \pm 0.57
	GN	67.38 \pm 0.61	68.13\pm0.34	67.63 \pm 0.56	66.34 \pm 1.39	68.31\pm0.76	66.89\pm0.78	68.01\pm0.95	68.49\pm0.39
disch_48h	LN	68.72\pm0.80	68.49 \pm 0.97	69.37 \pm 0.58	68.59\pm0.70	68.20 \pm 0.59	68.39\pm0.81	69.51\pm0.73	68.51 \pm 0.22
	GN	67.90 \pm 1.19	69.01\pm1.00	69.43\pm1.32	68.23 \pm 0.55	68.23\pm0.27	68.09 \pm 0.54	69.31 \pm 1.52	68.79\pm0.59
Acuity	LN	71.60 \pm 0.20	71.56 \pm 0.09	71.99 \pm 0.34	70.70\pm0.78	70.58\pm0.79	69.40\pm0.87	70.74 \pm 0.48	71.40 \pm 0.35
	GN	71.79\pm0.04	71.94\pm0.30	72.16\pm0.23	69.24 \pm 0.69	68.97 \pm 0.37	69.15 \pm 0.44	71.43\pm0.58	72.01\pm0.83
Average	LN	67.88	69.44	68.38	67.67	67.38	65.97	68	69.65
	GN	68.01	69.85	68.51	67.42	67.31	67.96	69.04	70.06

We present the results of the FL methods for six clinical prediction tasks on the eICU dataset described in Section 4.1. : mortality within 24 hours (mort_24h), mortality within 48 hours (mort_48h), length-of-stay (LOS), discharge within 24 hours (disch_24h), discharge within 48 hours (disch_48h), and final acuity prediction (Acuity). We present the experiment results using the data from the five largest clients with hospital IDs 73, 264, 420, 243, and 458 in Table 1.

Because there is no single method that consistently outperforms all other methods across all tasks, we averaged AUROC of all six tasks to determine the best performing model. We observe that most FL methods perform better when trained with GN instead of LN. We also observe that the average performance of our approach FedPxN trained using GN across all tasks is better than that of existing FL methods and our approach trained using LN. FedPxN also outperforms all FL methods in terms of AUPRC, which can be viewed on our GitHub repository [10].

Training with more clients We performed additional experiments in which we trained the FL methods with 10, 20, 30 largest clients and report the average AUROC of all six tasks. Table 2 reveals that GN outperforms LN in most FL methods trained with 5 – 30 clients. In addition, we observe that FedPxN yields the best AUROC in each setting (5, 10, 20, 30 clients) despite the similar monetary costs requirement of different FL methods. Note that the monetary cost of a FL method increases with the number of clients.

Testing on the top-5 client dataset We evaluated the performance of different FL methods on the test set from the five largest clients, while varying the number of clients on which the models were trained (*i.e.*, 5, 10, 20, 30). The performance is measured using average AUROC across all six tasks. The leftmost graph of Figure 3 shows that when the models by each FL method are trained with more clients (up to 20), the performances of all models trained with GN except FedYoGi and FedDyn are improved. In addition, the performance of FedProx continues to further improve up to 30 clients, which obtains the best performance. The second graph from the left of Figure 3 reveals that using up to 20 clients during training improves the performance of all methods with LN except for FedAdam and FedDyn. As for GN, the performance of FedProx with LN again increases further when it is trained with 30 clients. However, training FL with more clients means more expense from the perspective of service developers. Furthermore, we note that our approach yields the optimal performance and outperforms prior methods in most of the experiments.

Table 2: Average AUROC results for all six tasks for the eICU dataset using the data of the 5, 10, 20, 30 largest clients. For each FL method and each client setting, bold indicates the better normalization (LN or GN). We indicate the highest AUROC for each client setting in blue.

	5 clients		10 clients		20 clients		30 clients	
	LN	GN	LN	GN	LN	GN	LN	GN
FedAvg	67.88	68.01	67.34	67.7	68.62	68.87	67.52	68.06
FedProx	69.44	69.85	68.66	69.11	69.31	69.73	68.62	68.94
FedBN	68.38	68.51	68.24	68.19	69.21	69.3	68.43	68.13
FedAdam	67.67	67.42	67.8	67.87	68.09	68.96	67.67	68.1
FedAdagrad	67.38	67.31	67.31	67.68	67.98	68.85	67.3	67.61
FedYoGi	65.97	67.96	67.67	66.95	68.38	68.6	67.66	67.76
FedDyn	68	69.04	67.43	67.46	67.29	67.89	67.26	66.14
FedPxN	69.65	70.06	69.55	69.5	70.04	70.08	69.22	69.12

Testing on the top-30 client dataset We also evaluated all FL methods on the test set from the top 30 clients, while varying the number of clients the models were trained on. The performance is measured by the average AUROC of all six tasks. As depicted by two right-most graphs in Figure 3, the AUROC results of all methods except FedDyn consistently increase when both LN and GN are used. This demonstrates that training the model on more clients generalizes the model due to the availability of heterogeneous data and improves model performance. FedProx obtains the best performance with both GN and LN when the FL methods are trained on 20 or fewer clients. However, FedPxN yields the optimal performance when trained on the data of top 30 clients.

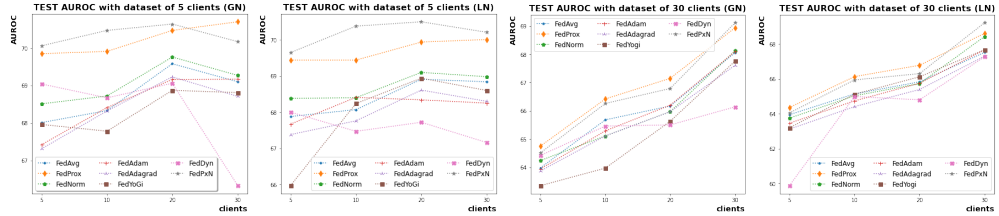


Figure 3: Test AUROC results for the five largest clients and all 30 clients measured using the models trained on varying numbers of clients.

5.2 Results for skin cancer images

Table 3: AUROC and AUPRC results for the skin cancer dataset using the data of five clients. Bold indicates the best normalization strategy (BN or GN) for each method. We indicate the best performance in blue.

	AUROC						AUPRC					
	Barcelona	Rosendahl	Vienne	UFES_brazil	SF_canada	Avg	Barcelona	Rosendahl	Vienne	UFES_brazil	SF_canada	Avg
FedAvg	BN 95.19±0.75	88.44±0.50	96.84±0.36	76.40±1.79	84.20±1.00	88.19±0.03	53.40±5.33	36.28±2.07	56.51±5.15	25.81±0.95	22.93±2.51	39.12±1.24
	GN 90.78±0.51	84.50±1.37	94.63±0.74	72.72±1.33	76.24±1.46	83.78±0.29	35.81±3.92	29.91±1.60	39.59±2.50	23.36±0.97	20.06±1.07	29.75±1.66
FedProx	BN 95.82±0.43	87.56±1.61	96.40±0.93	76.79±0.06	85.26±3.19	88.37±0.68	58.63±2.64	36.47±3.38	61.80±4.76	25.92±0.55	23.36±1.28	41.24±1.33
	GN 90.28±0.24	82.70±1.26	94.51±0.45	71.88±1.75	73.58±2.71	82.59±0.25	32.54±2.56	30.01±2.07	40.11±1.52	23.86±0.44	19.79±1.09	29.26±1.19
FedBN	BN 95.74±0.40	86.92±3.48	97.99±0.57	85.58±1.65	79.19±2.80	89.08±1.10	59.39±0.47	40.73±4.74	64.86±2.52	35.82±1.69	17.94±1.09	43.75±1.08
	GN 91.59±0.19	87.02±0.26	95.33±0.36	85.14±0.76	80.25±2.79	87.86±0.54	39.35±1.22	36.64±2.07	41.06±3.96	31.99±1.30	22.80±1.15	34.37±1.49
FedAdam	BN 64.50±3.55	65.53±2.89	68.50±2.40	64.64±2.24	71.46±9.06	66.93±2.00	13.70±0.39	17.88±1.26	14.74±0.16	18.17±0.84	17.55±1.03	16.41±0.66
	GN 91.97±0.26	80.63±1.83	95.22±0.55	70.65±2.14	75.77±1.10	82.85±0.32	40.34±6.00	29.47±1.30	42.68±2.69	24.39±1.13	20.32±1.16	31.44±2.29
FedAdagrad	BN 62.42±3.43	62.89±3.33	66.54±1.42	63.94±2.29	70.84±8.58	65.33±1.80	13.78±0.61	18.34±2.35	14.54±0.14	18.45±1.19	17.75±0.48	16.57±0.86
	GN 92.26±0.89	84.28±0.52	95.77±0.13	70.99±0.69	76.22±1.20	83.90±0.11	42.38±6.66	32.73±6.66	45.59±3.03	23.02±0.69	20.84±2.24	32.91±1.72
FedYoGi	BN 62.29±5.18	65.61±2.92	65.83±3.78	64.26±2.16	72.32±7.92	66.06±2.47	13.87±0.81	19.07±0.95	14.89±0.53	18.63±0.64	18.22±0.26	16.94±0.45
	GN 91.10±1.49	79.96±0.95	95.19±0.69	68.20±1.90	75.17±1.42	81.92±0.76	38.65±4.30	29.51±1.95	40.54±8.61	22.56±0.71	21.14±2.13	30.48±2.99
FedDyn	BN 80.75±0.85	83.45±0.62	91.98±0.42	72.62±1.20	85.61±0.92	82.88±0.68	20.73±0.53	24.14±0.21	21.20±0.29	23.55±0.46	21.27±0.22	22.18±0.09
	GN 88.42±0.14	86.35±1.12	95.47±0.18	82.73±0.98	82.19±1.07	87.03±0.72	28.03±1.11	30.51±1.16	41.38±3.58	31.93±1.03	20.60±1.06	30.71±1.04
FedPxN	BN 95.93±0.30	88.81±1.86	97.64±0.92	84.36±1.70	84.51±3.62	90.25±1.27	59.42±0.53	38.77±2.75	69.17±4.15	34.81±1.42	17.85±1.11	44.00±1.30
	GN 91.60±0.15	87.61±0.87	94.49±0.93	84.39±0.30	78.35±3.03	87.29±0.88	36.71±0.78	35.39±3.36	41.17±0.03	31.82±1.18	19.80±0.61	32.98±1.03

We present the results of FL methods on the skin cancer image dataset for the 8-way classification task with five clients for both BN and GN. Table 3 reveals that training with BN is better than GN in the FedAvg, FedProx, FedBN, and FedPxN when comparing clients' average AUROC and AUPRC results. In contrast, GN is better than BN in FedAdam, FedAdagrad, FedYoGi and FedDyn. Our approach, FedPxN, yields the overall best performance when trained with BN and GN. When using GN, FedBN also shows good performance when compared to other methods. Surprisingly, training

was extremely unstable when FedDyn was trained using BN. Specifically, a NaN value was found in the BN parameter during training. To address the problem, we tried 1) extensive hyper-parameter tuning, 2) allowing BN’s rescaling parameters to be aggregated [2] 3) allowing none of BN parameters to be aggregated [26], but none of the approaches helped improve the performance of FedDyn.

5.3 Result on ECG signals

Table 4: Test CinC scores for the ECG dataset using the data of the five clients. We indicate the best normalization strategy (BN or GN) for each method in bold. The highest average CinC is indicated in blue.

		Shaoxing	CSPC	Ga	Ningbo	PTBXL	Average
FedAvg	BN	65.8 ± 1.3	45.1 ± 1.0	39.0 ± 0.3	63.5 ± 1.0	13.1 ± 1.4	45.3 ± 0.4
	GN	65.4 ± 1.0	46.1 ± 0.4	37.6 ± 0.8	60.7 ± 0.2	11.1 ± 1.1	44.17 ± 0.6
FedProx	BN	66.9 ± 1.4	47.3 ± 0.8	40.0 ± 0.1	58.7 ± 0.9	14.7 ± 0.4	45.53 ± 0.5
	GN	65.3 ± 0.6	46.2 ± 0.1	37.1 ± 0.1	59.4 ± 1.0	10.4 ± 0.8	43.68 ± 0.1
FedBN	BN	78.9 ± 0.7	72.5 ± 0.8	46.5 ± 0.5	76.7 ± 0.3	52.2 ± 1.9	65.37 ± 0.3
	GN	77.6 ± 0.3	68.5 ± 1.5	49.2 ± 0.4	75.9 ± 0.5	49.7 ± 0.3	64.19 ± 0.3
FedAdam	BN	61.6 ± 1.3	43.9 ± 3.0	33.1 ± 1.6	56.9 ± 5.1	4.3 ± 1.3	39.95 ± 1.2
	GN	64.3 ± 1.1	44.7 ± 0.5	37.4 ± 1.0	60.5 ± 1.2	11.5 ± 0.9	43.67 ± 0.6
FedPxN	BN	78.0 ± 1.0	72.7 ± 0.3	51.7 ± 1.5	76.4 ± 0.5	55.8 ± 1.1	66.93 ± 0.1
	GN	78.4 ± 0.6	70.0 ± 1.1	48.7 ± 0.7	75.9 ± 0.5	51.8 ± 0.8	64.95 ± 0.4

We present the results of the FL methods for the 26 multi-label prediction task on ECG signals in Table 4. All the results indicate that training with BN is more effective in FedAvg, FedProx, FedBN and FedPxN whereas training with GN is better for FedAdam. Our proposed approach, FedPxN, shows overall the best performance based on average CinC score when trained with BN or GN. FedDyn failed to train with either BN or GN (similar to Section 5.2). To address this failure in training, we tried various modifications similar to those stated in Section 5.2. However, we still encountered failure in training. Therefore, we do not report the results of FedDyn.

5.4 Number of local epochs

We investigated the effect of the number of local epochs on the performance of the FL algorithms. We conducted experiments on the three datasets (eICU, skin cancer, and ECG) using 1, 5, and 10 local epochs, while fixing the number of total training epochs. The performance was averaged across three seeds. Figure 4 presents the results on the eICU dataset, where the images in the top and bottom rows show the plots of models trained with GN and LN, respectively. Each row contains four plots corresponding to models trained and tested on 5, 10, 20, and 30 clients by AUROC score averaged across all six tasks. Figure 5 presents the results of models trained with BN or GN and a varying number of local epochs on the skin cancer and ECG dataset. Figures 4 and 5 reveal that the performance of most FL methods including FedPxN consistently decreases as the number of local epochs increases. This demonstrates that FL methods perform well when fewer local epochs are used. Because the number of total training epochs is fixed, fewer local epochs indicate more communication rounds, which would require good internet connectivity and might result in increased bandwidth costs. However, in medicine, a model’s performance is the utmost priority, as it has a high impact on a patient’s life and a wrong prediction could lead to fatal errors. In addition, more communication rounds in FL in the medical domain is not a major problem, as the clients are hospitals that have LAN connections. Therefore, a better performing FL model is preferable in medicine.

5.5 Power consumption

We also measured the power consumed while conducting the experiments. The evaluated numbers of communication rounds and local epochs were (100, 1), (300, 1), and (200, 1), respectively, for the tasks on the eICU, skin cancer, and ECG datasets. We report the results for one seed value only for this experiment in Table 5. To understand the monetary costs of each method to achieve optimal performance, we conducted experiments using the normalization technique that showed better performance in Sections 5.1, 5.2, and 5.3. During training, we queried the NVIDIA System

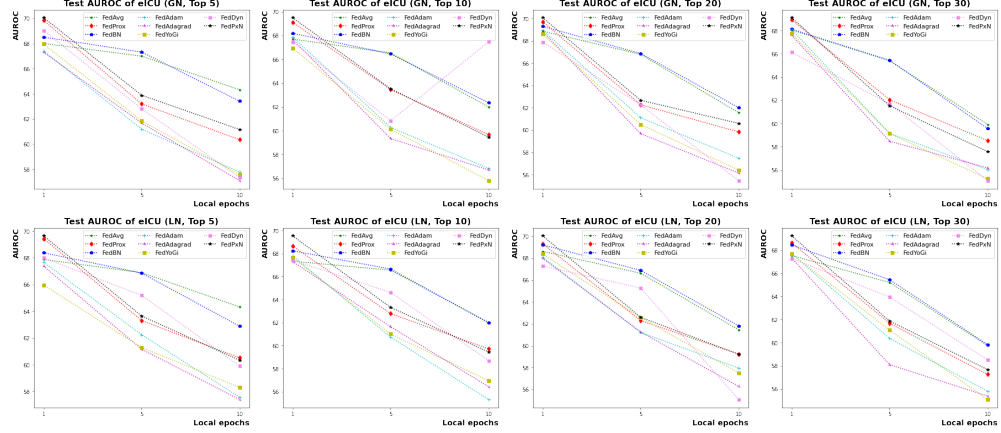


Figure 4: Test AUROC results for the eICU dataset as the number of local training epochs increases.

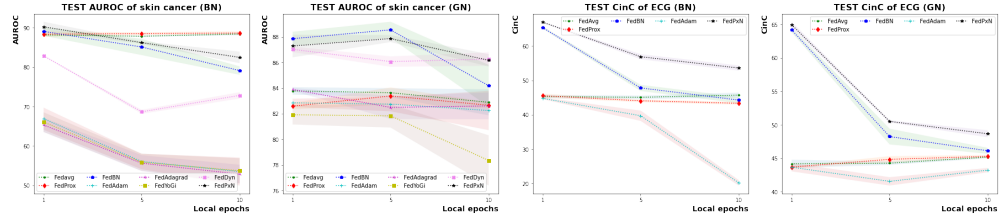


Figure 5: Test AUROC and CinC results for the skin cancer image and ECG datasets measured as the number of local training epochs increases.

Table 5: Power consumption of each method for the tasks in the eICU, skin cancer images, and ECG datasets. In eICU, we measured total power consumption of six tasks with 30 clients.

	FedAvg	FedProx	FedBN	FedPxN	FedAdam	FedAdagrad	FedYoGi	FedDyn
eICU								
	GN	GN	LN	LN	GN	GN	GN	LN
elapsed time (h)	5.66	5.82	4.51	4.51	4.81	4.84	5.14	5.13
Power consumption (kWh)	0.542	0.560	0.510	0.526	0.479	0.484	0.518	0.582
Skin cancer images								
	BN	BN	BN	BN	GN	GN	GN	GN
elapsed time (h)	10.53	10.62	10.29	10.27	10.56	10.67	10.61	9.49
Power consumption (kWh)	3.034	3.280	2.989	3.266	3.046	3.097	3.100	3.072
ECG								
	BN	BN	BN	BN	GN			
elapsed time (h)	9.14	11.49	9.15	10.71	9.58			
Power consumption (kWh)	2.955	3.484	2.888	3.401	3.016			

Management Interface ¹ at regular intervals to measure the power consumption of the GPU and averaged the measured values [42]. Then, we multiplied the obtained average values by elapsed time.

The power consumption of all FL methods is comparable. The difference between max and min power consumption among all methods in each dataset is between 0.103-0.596 kWh. The learning rate of FedAvg, FedProx, FedBN, and FedPxN, as well as the μ of FedProx and FedPxN have the same or similar values for the tasks on the three datasets. Therefore, if we perform a hyperparameter search of one method to obtain best value, we can use that value in other methods. However, FedOpt and FedDyn have a learning rate that is substantially different from those of the other methods. Moreover, there are more hyperparameters in FedOpt, such as η_g and, γ . Thus, the monetary costs of FedOpt and FedDyn are relatively higher than those of other methods because of the hyperparameter-tuning cost even if it is not shown on the table. Practically, FedBN is the cheapest technique for all tasks on the three datasets. The power consumption of FedPxN is 1.03-1.17 times more than that of FedBN.

¹<https://developer.nvidia.com/nvidia-system-management-interface>

6 Conclusion

In this work, we addressed the issue that IT companies, not hospitals, are primarily interested in FL when it comes to cross-silo FL in the clinical domain. Monetary cost and performance are the main concerns of these service providers. We conducted comprehensive experiments to study the performance of existing FL methods given a fixed budget with three massive medical datasets, each consisting of independent datasets from different sources. We also proposed a simple but effective algorithm, FedPxN, that introduces the regularization term from FedProx to the FedBN framework. It has a slightly higher power consumption than the most economical method, but consistently outperforms all other methods. We expect IT companies to refer to these experimental results to select suitable FL algorithm considering their clinical tasks and obtain stronger performance with lower costs. We also hope our research can raise more attention to FL in the clinical domain. An interesting future direction of our work is to extensively evaluate FedPxN across different clinical tasks (e.g., medical image segmentation). Further, reducing the power consumption of our approach would be another promising future direction.

References

- [1] Durmus Alp Emre Acar, Yue Zhao, Ramon Matas, Matthew Mattina, Paul Whatmough, and Venkatesh Saligrama. Federated learning based on dynamic regularization. In *International Conference on Learning Representations*, 2021.
- [2] Mathieu Andreux, Jean Ogier du Terrail, Constance Beguier, and Eric W Tramel. Siloed federated learning for multi-centric histopathology datasets. In *Domain Adaptation and Representation Transfer, and Distributed and Collaborative Learning*, pages 129–139. Springer, 2020.
- [3] Jimmy Lei Ba, Jamie Ryan Kiros, and Geoffrey E Hinton. Layer normalization. *arXiv preprint arXiv:1607.06450*, 2016.
- [4] Tariq Bdair, Nassir Navab, Shadi Albarqouni, et al. Semi-supervised federated peer learning for skin lesion classification. *Machine Learning for Biomedical Imaging*, 1(April 2022 issue):1–10, 2022.
- [5] Theodora S Brisimi, Ruidi Chen, Theofanie Mela, Alex Olshevsky, Ioannis Ch Paschalidis, and Wei Shi. Federated learning of predictive models from federated electronic health records. *International journal of medical informatics*, 112:59–67, 2018.
- [6] Bill Cassidy, Connah Kendrick, Andrzej Brodzicki, Joanna Jaworek-Korjakowska, and Moi Hoon Yap. Analysis of the isic image datasets: usage, benchmarks and recommendations. *Medical image analysis*, 75:102305, 2022.
- [7] Noel Codella, Veronica Rotemberg, Philipp Tschandl, M Emre Celebi, Stephen Dusza, David Gutman, Brian Helba, Aadi Kalloo, Konstantinos Liopyris, Michael Marchetti, et al. Skin lesion analysis toward melanoma detection 2018: A challenge hosted by the international skin imaging collaboration (isic). *arXiv preprint arXiv:1902.03368*, 2019.
- [8] Enmao Diao, Jie Ding, and Vahid Tarokh. Heterofl: Computation and communication efficient federated learning for heterogeneous clients. In *International Conference on Learning Representations*, 2020.
- [9] Qi Dou, Tiffany Y So, Meirui Jiang, Quande Liu, Varut Vardhanabhuti, Georgios Kaassis, Zeju Li, Weixin Si, Heather HC Lee, Kevin Yu, et al. Federated deep learning for detecting covid-19 lung abnormalities in ct: a privacy-preserving multinational validation study. *NPJ digital medicine*, 4(1):1–11, 2021.
- [10] Github. Github repository, 2022. URL https://github.com/wns823/medical_federated.
- [11] Wen Hao and Kang Jingsu. Investigating deep learning benchmarks for electrocardiography signal processing. *arXiv preprint arXiv:2204.04420*, 2022. doi: 10.48550/ARXIV.2204.04420.
- [12] Kevin Hsieh, Amar Phanishayee, Onur Mutlu, and Phillip Gibbons. The non-iid data quagmire of decentralized machine learning. In *International Conference on Machine Learning*, pages 4387–4398. PMLR, 2020.
- [13] Tzu-Ming Harry Hsu, Hang Qi, and Matthew Brown. Measuring the effects of non-identical data distribution for federated visual classification. *arXiv preprint arXiv:1909.06335*, 2019.
- [14] Li Huang, Andrew L Shea, Huining Qian, Aditya Masurkar, Hao Deng, and Dianbo Liu. Patient clustering improves efficiency of federated machine learning to predict mortality and hospital stay time using distributed electronic medical records. *Journal of biomedical informatics*, 99:103291, 2019.
- [15] Sergey Ioffe and Christian Szegedy. Batch normalization: Accelerating deep network training by reducing internal covariate shift. In *International conference on machine learning*, pages 448–456. PMLR, 2015.
- [16] Peter Kairouz, H Brendan McMahan, Brendan Avent, Aurélien Bellet, Mehdi Bennis, Arjun Nitin Bhagoji, Kallista Bonawitz, Zachary Charles, Graham Cormode, Rachel Cummings, et al. Advances and open problems in federated learning. *Foundations and Trends® in Machine Learning*, 14(1–2):1–210, 2021.
- [17] Jingsu Kang and Hao Wen. A study on several critical problems on arrhythmia detection using varying-dimensional electrocardiography. *Physiological Measurement*, 2022.
- [18] Sai Praneeth Karimireddy, Satyen Kale, Mehryar Mohri, Sashank Reddi, Sebastian Stich, and Ananda Theertha Suresh. Scaffold: Stochastic controlled averaging for federated learning. In *International Conference on Machine Learning*, pages 5132–5143. PMLR, 2020.
- [19] Jeremy Kawahara, Sara Daneshvar, Giuseppe Argenziano, and Ghassan Hamarneh. Seven-point checklist and skin lesion classification using multitask multimodal neural nets. *IEEE journal of biomedical and health informatics*, 23(2):538–546, 2018.

[20] Yejin Kim, Jimeng Sun, Hwanjo Yu, and Xiaoqian Jiang. Federated tensor factorization for computational phenotyping. In *Proceedings of the 23rd ACM SIGKDD International Conference on Knowledge Discovery and Data Mining*, pages 887–895, 2017.

[21] Diederik P Kingma and Jimmy Ba. Adam: A method for stochastic optimization. *arXiv preprint arXiv:1412.6980*, 2014.

[22] Geun Hyeong Lee and Soo-Yong Shin. Federated learning on clinical benchmark data: performance assessment. *Journal of medical Internet research*, 22(10):e20891, 2020.

[23] Qinbin Li, Yiqun Diao, Quan Chen, and Bingsheng He. Federated learning on non-iid data silos: An experimental study. In *IEEE International Conference on Data Engineering*, 2022.

[24] Tian Li, Anit Kumar Sahu, Manzil Zaheer, Maziar Sanjabi, Ameet Talwalkar, and Virginia Smith. Federated optimization in heterogeneous networks. *Proceedings of Machine Learning and Systems*, 2:429–450, 2020.

[25] Xiang Li, Kaixuan Huang, Wenhao Yang, Shusen Wang, and Zhihua Zhang. On the convergence of fedavg on non-iid data. In *International Conference on Learning Representations*, 2019.

[26] Xiaoxiao Li, Meirui Jiang, Xiaofei Zhang, Michael Kamp, and Qi Dou. Fed{bn}: Federated learning on non-{iid} features via local batch normalization. In *International Conference on Learning Representations*, 2021.

[27] Dianbo Liu, Timothy Miller, Raheel Sayeed, and Kenneth D Mandl. Fadl: Federated-autonomous deep learning for distributed electronic health record. *arXiv preprint arXiv:1811.11400*, 2018.

[28] Dianbo Liu, Dmitriy Dligach, and Timothy Miller. Two-stage federated phenotyping and patient representation learning. In *Proceedings of the conference. Association for Computational Linguistics. Meeting*, volume 2019, page 283. NIH Public Access, 2019.

[29] Ilya Loshchilov and Frank Hutter. Decoupled weight decay regularization. In *International Conference on Learning Representations*, 2018.

[30] Matthew McDermott, Bret Nestor, Evan Kim, Wancong Zhang, Anna Goldenberg, Peter Szolovits, and Marzyeh Ghassemi. A comprehensive ehr timeseries pre-training benchmark. In *Proceedings of the Conference on Health, Inference, and Learning*, pages 257–278, 2021.

[31] Brendan McMahan, Eider Moore, Daniel Ramage, Seth Hampson, and Blaise Aguera y Arcas. Communication-efficient learning of deep networks from decentralized data. In *Artificial intelligence and statistics*, pages 1273–1282. PMLR, 2017.

[32] Jungwoo Oh, Hyunseung Chung, Joon-myung Kwon, Dong-gyun Hong, and Edward Choi. Lead-agnostic self-supervised learning for local and global representations of electrocardiogram. In *Conference on Health, Inference, and Learning*, pages 338–353. PMLR, 2022.

[33] Andre GC Pacheco, Gustavo R Lima, Amanda S Salomão, Breno Krohling, Igor P Biral, Gabriel G de Angelo, Fábio CR Alves Jr, José GM Esgario, Alana C Simora, Pedro BC Castro, et al. Pad-ufes-20: a skin lesion dataset composed of patient data and clinical images collected from smartphones. *Data in brief*, 32:106221, 2020.

[34] Sangjoon Park, Gwanghyun Kim, Jeongsol Kim, Boah Kim, and Jong Chul Ye. Federated split task-agnostic vision transformer for COVID-19 CXR diagnosis. In A. Beygelzimer, Y. Dauphin, P. Liang, and J. Wortman Vaughan, editors, *Advances in Neural Information Processing Systems*, 2021.

[35] Tom J Pollard, Alistair EW Johnson, Jesse D Raffa, Leo A Celi, Roger G Mark, and Omar Badawi. The eicu collaborative research database, a freely available multi-center database for critical care research. *Scientific data*, 5(1):1–13, 2018.

[36] Sashank J Reddi, Zachary Charles, Manzil Zaheer, Zachary Garrett, Keith Rush, Jakub Konečný, Sanjiv Kumar, and Hugh Brendan McMahan. Adaptive federated optimization. In *International Conference on Learning Representations*, 2020.

[37] Matthew A Reyna, Nadi Sadr, Erick A Perez Alday, Annie Gu, Amit J Shah, Chad Robichaux, Ali Bahrami Rad, Andoni Elola, Salman Seyed, Sardar Ansari, et al. Will two do? varying dimensions in electrocardiography: the physionet/computing in cardiology challenge 2021. In *2021 Computing in Cardiology (CinC)*, volume 48, pages 1–4. IEEE, 2021.

[38] Tal Ridnik, Emanuel Ben-Baruch, Nadav Zamir, Asaf Noy, Itamar Friedman, Matan Protter, and Lihi Zelnik-Manor. Asymmetric loss for multi-label classification. In *Proceedings of the IEEE/CVF International Conference on Computer Vision (ICCV)*, pages 82–91, October 2021.

[39] Nicola Rieke, Jonny Hancox, Wenqi Li, Fausto Milletari, Holger R Roth, Shadi Albarqouni, Spyridon Bakas, Mathieu N Galtier, Bennett A Landman, Klaus Maier-Hein, et al. The future of digital health with federated learning. *NPJ digital medicine*, 3(1):1–7, 2020.

[40] Micah J Sheller, Brandon Edwards, G Anthony Reina, Jason Martin, Sarthak Pati, Aikaterini Kotrotsou, Mikhail Milchenko, Weilin Xu, Daniel Marcus, Rivka R Colen, et al. Federated learning in medicine: facilitating multi-institutional collaborations without sharing patient data. *Scientific reports*, 10(1):1–12, 2020.

[41] Huan Song, Deepta Rajan, Jayaraman J Thiagarajan, and Andreas Spanias. Attend and diagnose: Clinical time series analysis using attention models. In *Thirty-second AAAI conference on artificial intelligence*, 2018.

[42] Emma Strubell, Ananya Ganesh, and Andrew McCallum. Energy and policy considerations for deep learning in nlp. In *Proceedings of the 57th Annual Meeting of the Association for Computational Linguistics*, pages 3645–3650, 2019.

[43] Mingxing Tan and Quoc Le. Efficientnet: Rethinking model scaling for convolutional neural networks. In *International conference on machine learning*, pages 6105–6114. PMLR, 2019.

[44] Philipp Tschandl, Cliff Rosendahl, and Harald Kittler. The ham10000 dataset, a large collection of multi-source dermatoscopic images of common pigmented skin lesions. *Scientific data*, 5(1):1–9, 2018.

[45] Ashish Vaswani, Noam Shazeer, Niki Parmar, Jakob Uszkoreit, Llion Jones, Aidan N Gomez, Łukasz Kaiser, and Illia Polosukhin. Attention is all you need. *Advances in neural information processing systems*, 30, 2017.

[46] Jianyu Wang, Zachary Charles, Zheng Xu, Gauri Joshi, H Brendan McMahan, Maruan Al-Shedivat, Galen Andrew, Salman Avestimehr, Katharine Daly, Deepesh Data, et al. A field guide to federated optimization. *arXiv preprint arXiv:2107.06917*, 2021.

[47] Hao WEN and Jingsu KANG. torch_ecg: An ECG Deep Learning Framework Implemented using PyTorch, 2022. URL <https://zenodo.org/record/6435048>.

[48] Yuxin Wu and Kaiming He. Group normalization. In *Proceedings of the European conference on computer vision (ECCV)*, pages 3–19, 2018.

[49] Jie Xu, Zhenxing Xu, Peter Walker, and Fei Wang. Federated patient hashing. In *Proceedings of the AAAI Conference on Artificial Intelligence*, volume 34, pages 6486–6493, 2020.